

Anharmonicity-induced excited-state quantum phase transition in the two-dimensional limit of the vibron model

Jamil Khalouf-Rivera, Francisco Pérez-Bernal, and Miguel Carvajal*

*Dept. de Ciencias Integradas y Centro de Estudios Avanzados en Física,
Matemáticas y Computación, Unidad Asociada GIFMAN CSIC-UHU,*

Universidad de Huelva, Huelva 21071, SPAIN and

*Instituto Carlos I de Física Teórica y Computacional,
Universidad de Granada, Granada 18071, SPAIN*

(Dated: May 4, 2022)

Abstract

As already stated in *Phys. Rev. A* **81** 050101 (2010), the inclusion of anharmonicity into the 2D vibron model in the form of a quadratic bosonic number operator results in a second excited-state quantum phase transition. Such transition, in the classical limit of the model, can be associated with the lowering of the asymptotic energy of the energy functional. We delve into the nature of the new excited-state quantum phase transition and we characterize it in the previously overlooked symmetric phase of the model (also known as cylindrical oscillator or linear phase).

Quantum phase transitions (QPTs) are zero-temperature phase transitions that occur when a quantum system ground state (g.s.) undergoes an abrupt variation when a Hamiltonian interaction parameter, named *control parameter*, goes through a critical value. Such transitions have been observed in numerous quantum systems from different fields: quantum optics, condensed-matter, or atomic, nuclear, and molecular systems [1]. In the case of algebraic models, based on Lie algebras and useful in studies of molecular [2, 3], nuclear [4], and hadronic structure [5], the different phases can be mapped to the system dynamical symmetries (A general classification of ground state QPTs in algebraic models can be found in [6] and for an extended treatment see the reviews [7–9] and references therein).

In the present work we deal with the two-dimensional limit of the vibron model (2DVM), introduced by Iachello and Oss for the treatment of bending molecular vibrations [10] as collective bosonic excitations (vibrons). The dynamical algebra of the systems is $u(3)$, with two possible dynamical symmetries, associated with the $u(2)$ and $so(3)$ subalgebras and known as the cylindrical and anharmonic oscillator dynamical symmetries [11]. The two subalgebra chains end up in the system symmetry algebra, $so(2)$, which denotes the conservation of the vibrational angular momentum in the molecular case, a projection of the total angular momentum perpendicular to the plane of the bending motion

$$\begin{array}{ccc}
 & u(2) & \\
 & \nearrow \quad \searrow & \\
 u(3) & & so(2) . \\
 & \searrow \quad \nearrow & \\
 & so(3) &
 \end{array} \tag{1}$$

* Miguel Carvajal: miguel.carvajal@dfa.uhu.es

Each subalgebra chain has a corresponding basis set and a solvable Hamiltonian that can be mapped into a limiting physical case. In the molecular case, the $u(2)$ chain, known as the cylindrical oscillator chain, is associated with the bending degree of freedom in linear molecules and the $so(3)$ chain, known as the anharmonic oscillator chain, is associated with the bending of quasirigid bent molecules.

A very simple 2DVM Hamiltonian with only two interaction terms, the first-order Casimir of $u(2)$, \hat{n} , and the operator $\hat{P} = N(N+1) - \hat{W}^2$, where N is the system size and \hat{W}^2 is the second order Casimir of the $so(3)$ subalgebra

$$\hat{H} = (1 - \xi)\hat{n} + \frac{\xi}{N-1}\hat{P} . \quad (2)$$

We have fixed to unity an overall energy scale and the control parameter, $\xi \in [0, 1]$, brings the system from one limit to the other. In this case, the ground state of the system suddenly changes from the symmetric phase to the broken-symmetry phase in a second order ground state quantum phase transition, once the control parameter reaches the critical value $\xi_c = 0.2$ [12]. At $\xi = 0$, the 2DVM Hamiltonian recovers the linear limit, whereas for $\xi = 1$, a pure bent Hamiltonian is obtained. In the intermediate value of $\xi_c = 0.2$, the system exhibits a QPT, when ξ takes values below the critical point, ξ_c , the bending mode behaves as for a linear molecule whereas the region of nonrigid and semirigid bent molecules corresponds to the values $\xi_c < \xi \leq 1$. It is in this latter region that the ESQPT can emerge [13–15] and, therefore, the excited energy levels can undergo the bent-to-linear transition when moving upward in energy. A functional form of the separatrix line, that marks the energy with a high local density of states, can be obtained from the classical bending energy functional obtained using the coherent state formalism [12].

Though the abrupt change that characterizes a QPT is only possible in the large system size limit (also called thermodynamical or mean field limit), even for finite system sizes the critical point can be identified by QPT precursors under the form of sharp changes in several quantities, e.g. the energy gap collapse between consecutive levels, the increase in the energy density, sudden changes in the participation ratio, or the Wehrl entropy [16–21].

In more recent times, the study of QPTs has been brought to the realm of excited states with the so-called excited state quantum phase transitions (ESQPTs) [22, 23]. In ESQPTs, for a fixed value of the control parameter, a non-analiticity in a certain derivative of the density of energy levels is found at a critical energy value [24–28]. Eigenstates below and

above the critical energy are considered to belong to different phases. Therefore, ESQPTs can be accessed in two different ways: varying the control parameter and tracing the changes of a given eigenstate once it goes through the critical energy value; or fixing the control parameter and examining the properties of eigenstates at increasing energy values. ESQPTs have been studied in different models, e.g., the nuclear interacting boson model [8], the Jaynes-Cummings model [29], the kicked-top model [30], the Rabi [31] and Dicke [17, 29, 32, 33] models, and the Lipkin-Meshkov-Glick (LMG) model [8, 34–38]. For a recently published review of this field, see Ref. [28] and references therein.

The 2DVM is the simplest two-level model with a nontrivial angular momentum. This explains why it has been instrumental in the definition of ESQPTs from the onset [23]. The connection between the phenomenon of quantum monodromy and the ESQPT in the 2DVM [12] is also a relevant aspect. Nonrigid molecules are characterized by the existence of a barrier-to-linearity in the bending potential that is low enough to be straddled by excited states. This results in a large amplitude bending mode and a feature-rich spectroscopy [39], with a sign-changing anharmonicity (Dixon dip [40]) and a dependence of energy on vibrational angular momentum that changes from quadratic to linear as the excitation energy goes through the barrier-to-linearity [41–43]. Mexican hat or Champagne bottle type potentials have been used for the modeling of nonrigid species, and the presence of the barrier to linearity prevents the definition of a set of globally valid action-angle variables [44]. When this classical feature is translated into the quantum realm, the result is known as quantum monodromy, and precludes the definition of a unique set of vibrational quantum numbers globally valid for the system [41, 45]. Quantum monodromy has helped in the assignment of quantum labels to experimental bending spectra of nonrigid molecular species [42, 46–51].

In addition to the two limiting physical cases, the 2DVM model can also tackle the feature-rich bending spectrum of nonrigid cases [52, 53]. This model has also been combined with others to deal with coupled benders [54–56] or coupling between bending and stretching degrees of freedom [57–60].

It is worth to emphasize that the bending vibration of nonrigid molecules is the first physical system where ESQPT signatures have been identified in experimental data, with a close connection between quantum monodromy and the 2DVM ESQPT. Hence, the algebraic approach has proved to be an efficient tool in the modeling of nonrigid molecular species [14, 43, 61]. In most cases, fits have been performed using a 2DVM Hamiltonian that includes

up to two-body interactions. The authors have recently explored the improvement in the agreement with reported bending spectra for several molecular species obtained using the most general 2DVM Hamiltonian including up to four-body interactions [14]. Other systems where signatures of ESQPTs have been detected in experimental results are superconducting microwave billiards [62] and spinor Bose-Einstein condensates [63].

Considering the advances in molecular spectroscopy and the accuracy of the observed vibrational spectra, the fit to experimental accuracy of reported bending band origins with the 2DVM requires a Hamiltonian beyond the model Hamiltonian (2), including higher order interactions. The authors have recently published a set of calculations for different the bending spectrum of several molecular species of interest using the most general four-body 2DVM Hamiltonian [14, 64], obtaining very satisfactory results.

The addition of higher-order interactions to the model Hamiltonian (2) substantially modifies the model ESQPT, as shown in Ref. [13] where the effects of the inclusion of an anharmonic term (quadratic correction $\hat{n}(\hat{n} + 1)$) were examined in the broken-symmetry phase. The obtained results include a substantially altered excited state energy density that fosters the appearance of a second critical energy line (separatrix) marked by a high level density. Recently, in the framework of a study of the transition state in isomerization reactions [64], we have noticed that the inclusion of a anharmonic term $\hat{n}(\hat{n} + 1)$ with a negative parameter in the Hamiltonian triggers an ESQPT in the symmetric region. In Ref. [13] the new ESQPT was analyzed only the broken symmetry phase ($\xi > 0.2$) as this is the region that hosted the bent-to-linear ESQPT. A full understanding of the new ESQPT is the main motivation for the present article. In this case, it is important to emphasize that the ESQPT is not associated with a saddle point or a local maximum in the potential, as it is the case in the ESQPT associated with the barrier to linearity and quantum monodromy [14]. The new ESQPT can be traced back to the changes that the anharmonic term brings about the phase-space boundary of the finite-dimensional Hilbert space [27, 28], which makes the present system a particularly interesting one.

Therefore, our starting point, the same than in Ref. [13], is the model Hamiltonian (2) plus a two-body interaction $\hat{n}(\hat{n} + 1)$ and the corresponding control parameter, α

$$\hat{H} = (1 - \xi)\hat{n} + \frac{\alpha}{N - 1}\hat{n}(\hat{n} + 1) + \frac{\xi}{N - 1}\hat{P} . \quad (3)$$

The new control parameter is α and, as in Ref. [13], we are interested in the negative values

of this parameter. As the new interaction is of a two-body nature, we scale it by a $N - 1$ factor to transform the Hamiltonian into an intensive form and facilitate the calculations in the large system size (mean field) limit. The energy functional of the system's Hamiltonian (3), obtained in the mean field limit and using the number-projected coherent (or intrinsic) state approach [12, 13], is

$$\mathcal{E}(r) = (1 - \xi) \frac{r^2}{1 + r^2} + \alpha \frac{r^4}{(1 + r^2)^2} + \xi \left(\frac{1 - r^2}{1 + r^2} \right)^2 \quad (4)$$

A Landau analysis of the ground state QPT for the model Hamiltonian (2) was performed in Ref. [12] and for the Hamiltonian with the anharmonic term in Ref. [13], though in this last case the analysis was limited to the bent or broken symmetry phase ($\xi_c = 0.2 < \xi < 1$) where two ESQPTs and the corresponding separatrices, that provide the critical energy for the ESQPT expressed as normalized excitation energies $((E - E_{gs})/N)$

$$f_1^{ESQPT}(\xi) = \frac{(5\xi - 1)^2}{16\xi}, \quad (5)$$

$$f_2^{ESQPT}(\xi, \alpha) = \frac{(3\xi + 2\alpha + 1)}{4(4\xi + \alpha)}. \quad (6)$$

The first separatrix, $f_1^{ESQPT}(\xi)$, depends only on the ξ control parameter and is associated with the barrier to linearity. However, the second one, $f_2^{ESQPT}(\xi, \alpha)$, depends on the α control parameter and can be traced back to the changes in the boundary of the phase space through the influence of α over the asymptotic values of the energy functional (4).

As we are currently interested in the extension of the results to the symmetric phase ($0 \leq \xi \leq \xi_c = 0.2$), we depict in Fig. 1 the excitation energy for vibrational angular momenta $\ell = 0$ (blue continuous line) and 1 (red dashed line) versus the control parameter ξ in this region. In this figure it can be clearly seen how the ground state QPT occurs at $\xi = \xi_c = 0.2$ and the onset of the bent-to-linear ESQPT with its associated separatrix $f_1^{ESQPT}(\xi)$ separatrix. The ESQPT associated to the anharmonicity and its separatrix $f_2^{ESQPT}(\xi, \alpha)$ occurs at higher energies and is also present for control parameter values $0 \leq \xi \leq \xi_c = 0.2$, with a high level density region and displaying the expected degeneracy of states with different vibrational angular momentum above the separatrix: states below the $f_1^{ESQPT}(\xi)$ and above the $f_2^{ESQPT}(\xi, \alpha)$ ESQPT separatrices are degenerate, while this degeneracy is broken for state in-between both separatrices.

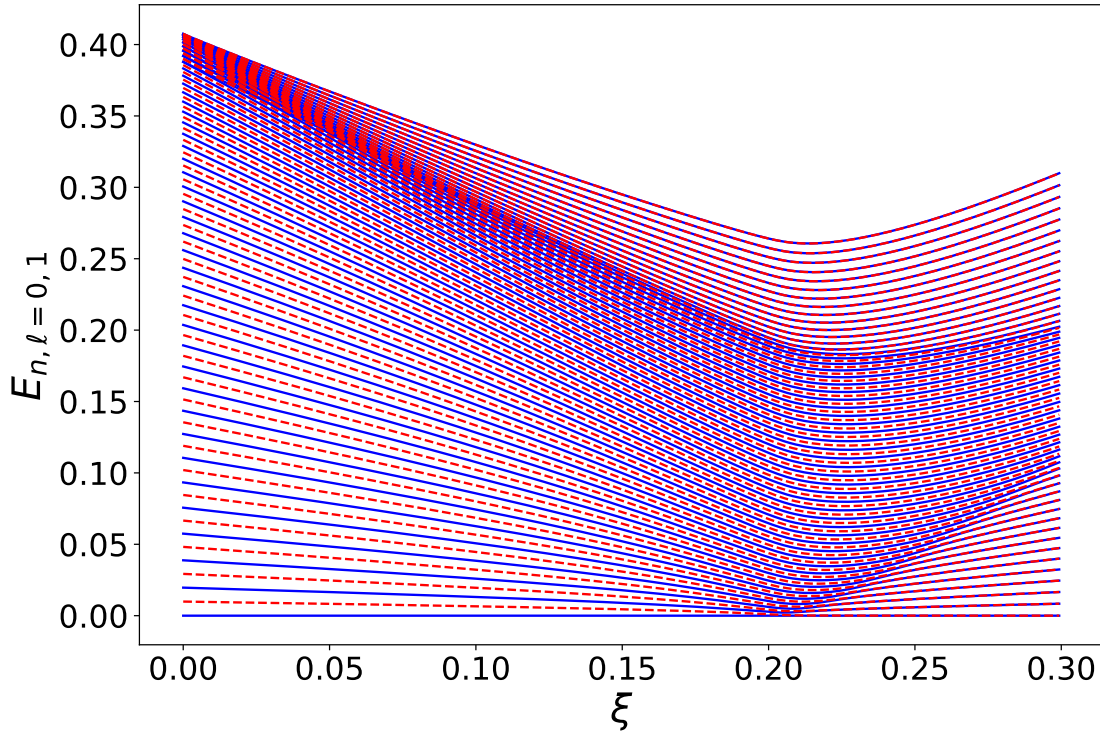


FIG. 1. Normalized excitation energy, $E_{n,\ell}$, for vibrational angular momentum $\ell = 0, 1$, as a function of the control parameter ξ for a $\alpha = -0.6$ and a system size $N = 100$. The $\ell = 0$ (1) energies are depicted using blue full (red dashed) lines.

A threshold value of α , α_t in the symmetric region ($0 < \xi < \xi_c$) can be obtained applying the maximum condition to the energy functional (4) out of the origin ($r \neq 0$):

$$\left. \frac{\partial \mathcal{E}(r)}{\partial r} \right|_{r \neq 0} = 0 \longrightarrow r^2 = \frac{5(\xi - \xi_c)}{-2|\alpha| + (3\xi + 1)} . \quad (7)$$

The minimum value of α is such that there is no other extreme but the one in the origin, which translates into a constraint in the absolute value of the control parameter: $|\alpha| < |\alpha_t|$. As we are interested in the $0 \leq \xi \leq \xi_c$, the numerator of (7) is zero or negative. Hence, we impose the condition $-2|\alpha| + (3\xi + 1) > 0$, obtaining a threshold value $|\alpha_t| = \frac{3\xi+1}{2}$. Therefore, the range of α values with a single minimum at the origin, characteristic of the symmetric phase or a linear molecular configuration in bending vibrations, is given by $-\frac{3\xi+1}{2} < \alpha < 0$. This is shown in Fig. 2, where various energy functionals (4), for a fixed $\xi = 0.1$, and different values of α are shown. Apart from the threshold value α_t (black dashed line) also the $\alpha = 0$

(red line), $\alpha = 0.5\alpha_t$ (blue line), and $\alpha_3 = 1.5\alpha_t$ (green line) are depicted. From this figure it is clear how for increasing α values the asymptotic energy functional value is lowered and the existence of a second extreme, a maximum at $r \neq 0$, appears for $|\alpha| > |\alpha_t|$. In the present work, we will only address the case $|\alpha| < |\alpha_t|$, that has been found a realistic approach to the highly excited states of linear molecules in the presence of bond-breaking isomerization [64].

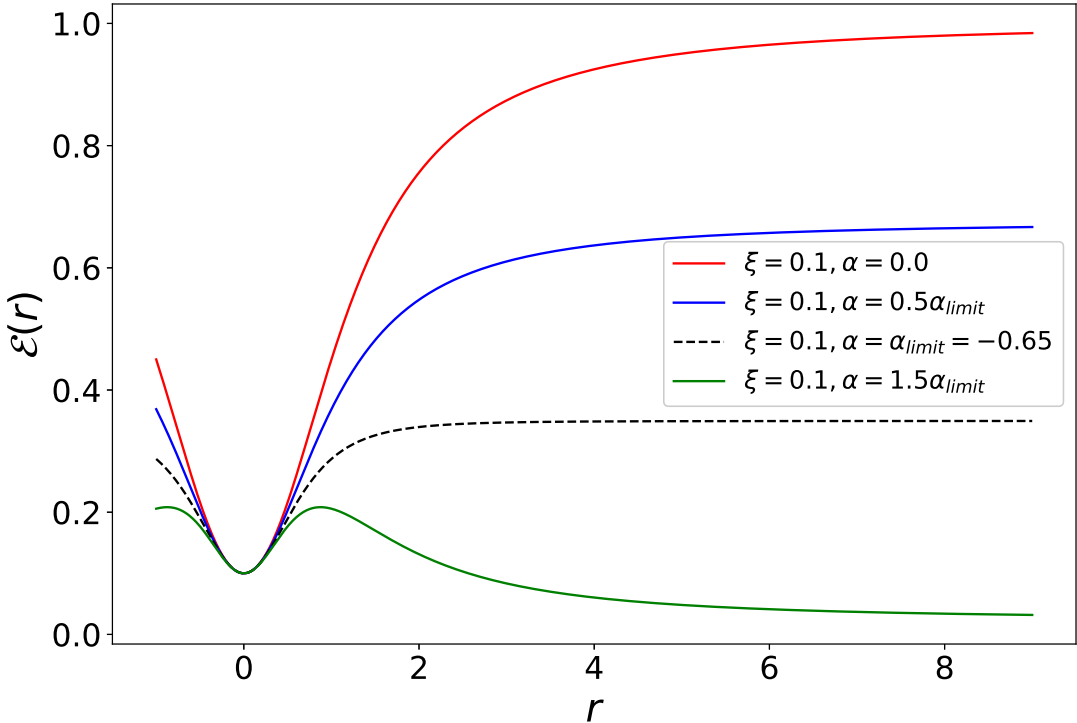


FIG. 2. Energy functionals for the Hamiltonian of Eq. (3) with a control parameter $\xi = 0.1$ and a α : $\alpha_1 = 0$ (red line), $\alpha_2 = 0.5\alpha_t$ (blue line), $\alpha = \alpha_t$ (black dashed line), and $\alpha_3 = 1.5\alpha_t$ (green line).

The analysis of the classical energy functional allows us to define the separatrix of the ESQPT in the symmetric phase, as the energy difference between the minimum value - located at $r = 0$ in this phase- and the asymptotic value of the the functional (4) (see Fig. 2)

$$f_3^{\text{ESQPT}}(\xi, \alpha) = \mathcal{E}(\infty) - \mathcal{E}(0) = 1 - \xi + \alpha . \quad (8)$$

The ESQPT in the symmetric phase can be studied using physical quantities such as the effective frequency, defined as $\omega_{n,\ell}^{eff} = \Delta E_{n,\ell}/\Delta n$ [64, 65], or the expectation value of the quantum number \hat{n} in the system eigenstates. The latter quantity acts as an order parameter for the ground state QPT [12]. Both quantities are depicted in Fig. 3 for system sizes $N = 50, 100$ and 1000 , control parameter $\xi = 0.19$, and anharmonicity parameter values $\alpha = -0.55, -0.65$ and -0.75 . In the left panel $\omega_{n,\ell}^{eff}$ is displayed versus the mean excitation energy between adjacent states, $(\bar{E}_{n,\ell})$, which is akin to a Birge-Sponer diagram. In this quantity, a deep minimum marks the critical ESQPT energy $f_3^{\text{ESQPT}}(\xi, \alpha)$ (8) for each α value. The second quantity is depicted in the right panel as a function of the eigenstate energy, with sharp maxima at the critical energy values. These features are sharper the larger the considered system size, but clear precursors of the ESQPT are found even for low N values.

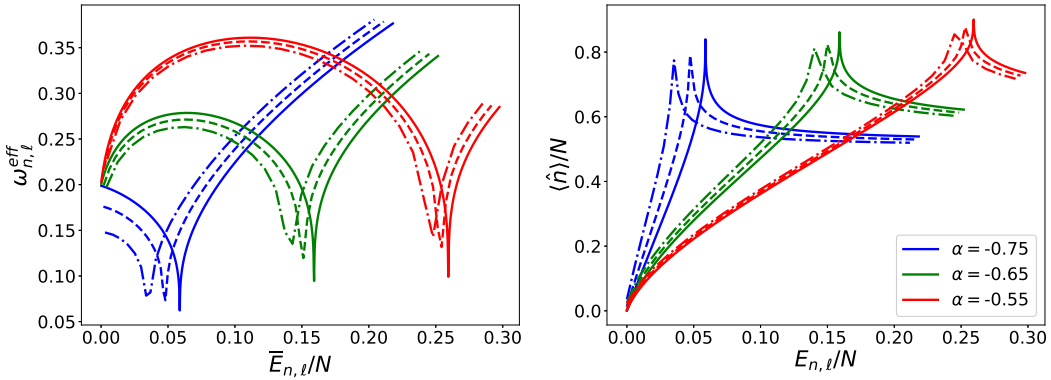


FIG. 3. Left panel: effective frequency $\omega_{n,\ell=0}^{eff}$ versus the mean value of the normalized excitation energy for $\ell = 0$ states. Right panel: expected value of \hat{n} in the system $\ell = 0$ eigenstates versus the normalized excitation energy. The calculations in both panels are carried out for Hamiltonian (3) with $N = 50, 100$ and 1000 , $\xi = 0.19$, and different α values (see legend).

As shown for the different limits of the vibron model in Refs. [66–68], the eigenstates closer to the critical energy in ESQPTs associated with a $u(n) - so(n+1)$ ground state quantum phase transition are strongly localized in the $u(n)$ basis. In the 2DVM case, the localization of a given state expressed in the $u(2)$, $\psi = \sum_{n,\ell} C_n |n^\ell\rangle$, can be assessed using the

participation ratio (PR) [69, 70]

$$P(\psi) = \frac{1}{\sum_{n,\ell} |C_{n,\ell}|^4} . \quad (9)$$

In the ESQPT associated with the barrier to linearity, the closest to the critical energy states are strongly localized, having a large component for the $|[N]0^0\rangle$ basis state [14, 15, 68]. We illustrate in Fig. 4 the eigenstate structure, selecting several cases for Hamiltonian (3) with $\xi = 0.19$, $\alpha = -0.7$, and a system size $N = 800$. In the three first rows of the figure we plot the squared coefficients, $|C_{n,\ell=0}^j|^2$, for an $\ell = 0$ eigenfunction below the ESQPT critical energy (first row, 101-th eigenstate), closest to the critical energy (second row, 209-th eigenstate), and above the critical energy (third row, 301-st eigenstate). The left column panels depict the squared coefficients as a function of the normalized $u(2)$ quantum number, n/N , and the right column as a function of the expectation value of the Hamiltonian for the corresponding basis state, $\langle [N] n^{\ell=0} | \hat{H} | [N] n^{\ell=0} \rangle / N$. It is evident that the eigenstate close to the separatrix is significantly more localized than the eigenstates below and above. In particular, and as it was already noticed in Ref. [14], the localization is achieved in the $|n^0\rangle = |N^0\rangle$ basis state (assuming N is even).

In the bottom row panels of Fig. 4, we depict the normalized PR, $P(\psi)/N$, for all eigenstates of the above mentioned case versus the quantum number n/N (left panel) and versus the energy per particle (right panel). The lower the PR value, the higher the state localization. As expected, states close to the ground state or the maximum energy are well located in this basis; particularly the first state, which has a high component in $|[N]0^0\rangle$. In between the two boundaries, there is a third minimum PR value, that occurs for states closer to the ESQPT critical energy.

In conclusion, we have shown that the ESQPT associated to the anharmonicity in the 2DVM extends to the symmetric phase. We present a threshold value for the anharmonicity α and we have derived, using the intrinsic state formalism, the dependence of the separatrix in the symmetric phase for the ESQPT (see Eq. 8). We have also depicted the operator used as a ground state order parameter, the expectation value of \hat{n} , the effective frequency (Birge-Sponer) plot, and we have shown the high degree of localization of the eigenfunctions closest to the critical energy in the linear basis. This Hamiltonian has been further extended with higher order interactions and used to model the HCN-HNC isomerization process, identifying the present ESQPT with the transition state, and the delocalization of the where

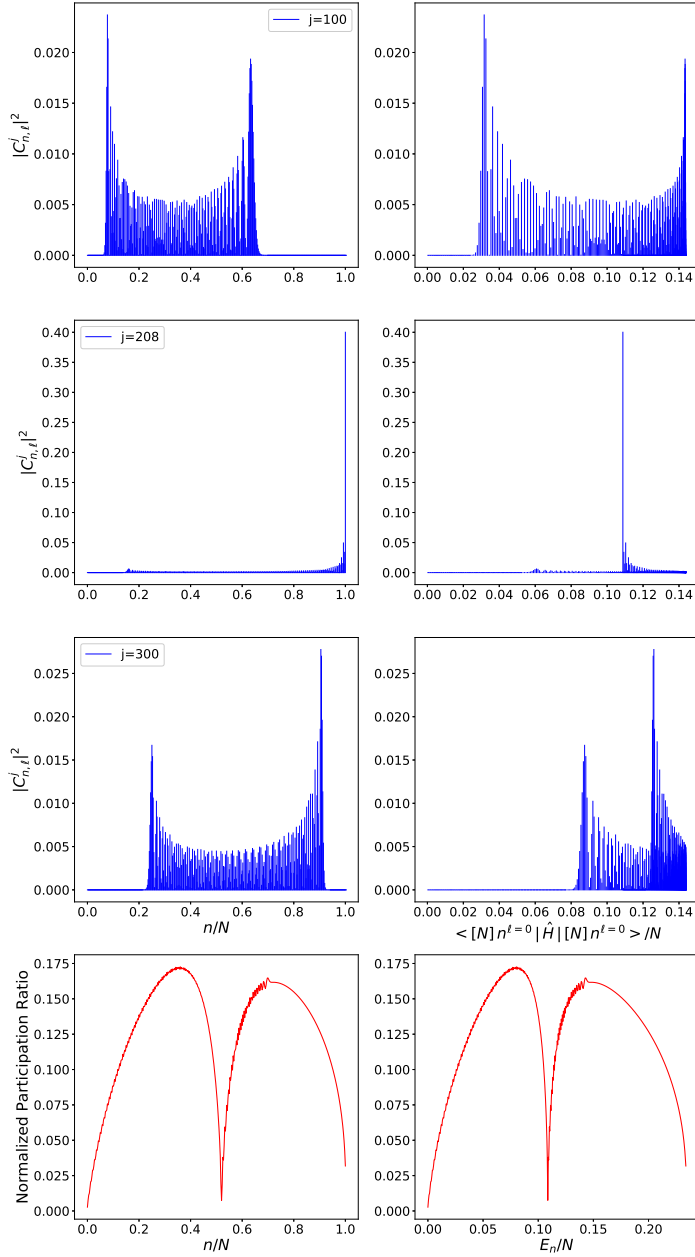


FIG. 4. The three first rows display the squared components of the $j = 100$ (first row), 208 (second row), and $j = 300$ eigenstates expressed in the $U(2)$ basis. Components are plotted versus n/N (left panels) and the diagonal matrix elements of the Hamiltonian in the corresponding basis (right panel). The last row shows the normalized participation ratio in the $U(2)$ basis versus n/N and versus the normalized energy. All cases: Hamiltonian (3) with parameter values $\xi = 0.19$, $\alpha = -0.7$ and system size $N = 800$.

the hydrogen atom with respect to the chemical bond C-N [64].

ACKNOWLEDGMENTS

This project has received funding from the European Union’s Horizon 2020 research and innovation program under the Marie Skłodowska-Curie grant agreement No 872081 and from the Spanish National Research, Development, and Innovation plan (RDI plan) under the project PID2019-104002GB-C21. This work has also been partially supported by the Consejería de Conocimiento, Investigación y Universidad, Junta de Andalucía and European Regional Development Fund (ERDF), ref. SOMM17/6105/UGR (FPB and MC), UHU-1262561 (JKR and FPB) and by the Ministerio de Ciencia, Innovación y Universidades (ref.COOPB20364) (MC). Computing resources supporting this work were provided by the CEAFCM and Universidad de Huelva High Performance Computer (HPC@UHU) located in the Campus Universitario el Carmen and funded by FEDER/MINECO project UNHU-15CE-2848.

- [1] L. Carr. *Understanding Quantum Phase Transitions*. Condensed Matter Physics. CRC Press, 2010.
- [2] F. Iachello and R.D. Levine. *Algebraic Theory of Molecules*. Oxford University Press, New York, 1995.
- [3] A. Frank and P. Van Isacker. *Algebraic Methods in Molecular and Nuclear Structure Physics*. John Wiley and Sons, New York, 1994.
- [4] F. Iachello and A. Arima. *The Interacting Boson Model*. Cambridge University Press, Cambridge, 1987.
- [5] R. Bijker, F. Iachello, and A. Leviatan. Algebraic Models of Hadron Structure. I. Nonstrange Baryons . *Ann. Phys.*, 236:69 – 116, 1994.
- [6] P. Cejnar and F. Iachello. Phase structure of interacting boson models in arbitrary dimension. *J. Phys. A: Math. and Theor.*, 40:581, 2007.
- [7] R.F. Casten. Quantum phase transitions and structural evolution in nuclei. *Prog. Part. Nucl. Phys.*, 62(1):183–209, 2009.
- [8] Pavel Cejnar and Jan Jolie. Quantum phase transitions in the interacting boson model. *Prog. Part. Nucl. Phys.*, 62(1):210–256, 2009.

[9] Pavel Cejnar, Jan Jolie, and Richard F. Casten. Quantum phase transitions in the shapes of atomic nuclei. *Rev. Mod. Phys.*, 82:2155–2212, Aug 2010.

[10] F. Iachello and S. Oss. Algebraic approach to molecular spectra: Two dimensional problems. *J. Chem. Phys.*, 104:6956–6963, 1996.

[11] There exists a third chain known as $\overline{so(3)}$, but it does not introduce any new feature [12].

[12] F. Pérez-Bernal and F. Iachello. Algebraic approach to two-dimensional systems: Shape phase transitions, monodromy, and thermodynamic quantities. *Phys. Rev. A*, 77:032–115, 2008.

[13] F. Pérez-Bernal and O. Álvarez-Bajo. Anharmonicity effects in the bosonic $u(2)$ - $so(3)$ excited-state quantum phase transition. *Phys. Rev. A*, 81:050–101, 2010.

[14] Jamil Khalouf-Rivera, Francisco Pérez-Bernal, and Miguel Carvajal. Excited state quantum phase transitions in the bending spectra of molecules. *J. Quant. Spectrosc. and Rad. Transfer*, 261:107436, 2021.

[15] Jamil Khalouf-Rivera, Miguel Carvajal, and Francisco Pérez-Bernal. Quantum fidelity susceptibility in excited state quantum phase transitions: application to the bending spectra of nonrigid molecules. 2021.

[16] Y. Zhang, F. Pan, Y.-X. Liu, and J.P. Draayer. The $e(2)$ symmetry and quantum phase transition in the two-dimensional limit of the vibron model. *J. Phys. B – At. Mol. Opt.*, 43:225101, 2010.

[17] P. Pérez-Fernández, J.M. Arias, J. E. García-Ramos, and F. Pérez-Bernal. Finite-size corrections in the bosonic algebraic approach to two-dimensional systems. *Phys. Rev. A*, 83:062125, 2011.

[18] M Calixto, E Romera, and R del Real. Parity-symmetry-adapted coherent states and entanglement in quantum phase transitions of vibron models. *J. Phys. A: Math. Theor.*, 45:365301, 2012.

[19] M. Calixto, R. del Real, and E. Romera. Husimi distribution and phase-space analysis of a vibron-model quantum phase transition. *Phys. Rev. A*, 86:032508, 2012.

[20] F. de los Santos and E. Romera. Revival times at quantum phase transitions. *Phys. Rev. A*, 87:013424, 2013.

[21] O. Castaños, M. Calixto, F. Pérez-Bernal, and E. Romera. Identifying the order of a quantum phase transition by means of wehrl entropy in phase space. *Phys. Rev. E*, 92:052106, 2015.

[22] P. Cejnar, M. Macek, S. Heinze, J. Jolie, and J. Dobeš. Monodromy and excited-state quantum

phase transitions in integrable systems: Collective vibrations of nuclei. *J. Phys. A: Math. and General*, 39:L515–L521, 2006.

[23] M.A. Caprio, P. Cejnar, and F. Iachello. Excited State Quantum Phase Transitions in Many-Body Systems. *Ann. Phys.*, 323:1106 – 1135, 2008.

[24] P. Cejnar and P. Stransky. Impact of quantum phase transitions on excited-level dynamics. *Phys. Rev. E*, 78, 2008.

[25] Pavel Stránský, Michal Macek, and Pavel Cejnar. Excited-State Quantum Phase Transitions in Systems with Two Degrees of Freedom: Level Density, Level Dynamics, Thermal Properties. *Ann. Phys.*, 345:73 – 97, 2014.

[26] Pavel Stránský, Michal Macek, Amiram Leviatan, and Pavel Cejnar. Excited-State Quantum Phase Transitions in Systems with Two Degrees of Freedom: II. Finite-Size Effects. *Ann. Phys.*, 356:57 – 82, 2015.

[27] Michal Macek, Pavel Stránský, Amiram Leviatan, and Pavel Cejnar. Excited-state quantum phase transitions in systems with two degrees of freedom. iii. interacting boson systems. *Phys. Rev. C*, 99:064323, Jun 2019.

[28] Pavel Cejnar, Pavel Stránský, Michal Macek, and Michal Kloc. Excited-state quantum phase transitions. *J. Phys. A: Mathem. and Theoret.*, 2021.

[29] P. Pérez-Fernández, A. Relaño, J. M. Arias, P. Cejnar, J. Dukelsky, and J. E. García-Ramos. Excited-state phase transition and onset of chaos in quantum optical models. *Phys. Rev. E*, 83:046208, 2011.

[30] V.M. Bastidas, P. Pérez-Fernández, M. Vogl, and T. Brandes. Quantum criticality and dynamical instability in the kicked-top model. *Phys. Rev. Lett.*, 112:140408, 2014.

[31] Ricardo Puebla, Myung-Joong Hwang, and Martin B. Plenio. Excited-state quantum phase transition in the rabi model. *Phys. Rev. A*, 94:023835, Aug 2016.

[32] T. Brandes. Excited-state quantum phase transitions in Dicke superradiance models. *Phys. Rev. E*, 88:032133, 2013.

[33] Michal Kloc, Pavel Stránský, and Pavel Cejnar. Quantum quench dynamics in dicke superradiance models. *Phys. Rev. A*, 98:013836, Jul 2018.

[34] P. Pérez-Fernández, A. Relaño, J. M. Arias, J. Dukelsky, and J. E. García-Ramos. Decoherence due to an excited-state quantum phase transition in a two-level boson model. *Phys. Rev. A*, 80:032111, 2009.

[35] Z.-G. Yuan, P. Zhang, S.-S. Li, J. Jing, and L.-B. Kong. Scaling of the berry phase close to the excited-state quantum phase transition in the Lipkin model. *Phys. Rev. A*, 85:044102, 2012.

[36] Wassilij Kopylov and Tobias Brandes. Time delayed control of excited state quantum phase transitions in the lipkin–meshkov–glick model. *New J. Phys.*, 17(10):103031, oct 2015.

[37] Qian Wang and Francisco Pérez-Bernal. Excited-state quantum phase transition and the quantum-speed-limit time. *Phys. Rev. A*, 100:022118, Aug 2019.

[38] Qian Wang and Francisco Pérez-Bernal. Probing an excited-state quantum phase transition in a quantum many-body system via an out-of-time-order correlator. *Phys. Rev. A*, 100:062113, Dec 2019.

[39] W. Quapp and B.P. Winnewisser. What you thought you already knew about the bending motion of triatomic molecules. *J. Math. Chem.*, 14:259–285, 1993.

[40] R. N. Dixon. Higher Vibrational Levels of a Bent Triatomic Molecule. *Trans. Faraday Soc.*, 60:1363–1368, 1964.

[41] M. S. Child. Quantum states in a champagne bottle. *J. Phys. A: Math. and General*, 31:657–670, 1998.

[42] M. Winnewisser, B.P. Winnewisser, I.R. Medvedev, F.C. De Lucia, S.C. Ross, and L.M. Bates. The Hidden Kernel of Molecular Quasi-Linearity: Quantum Monodromy. *J. Mol. Struct.*, 798:1 – 26, 2006.

[43] D. Larese and F. Iachello. A Study of Quantum Phase Transitions and Quantum Monodromy in the Bending Motion of Non-Rigid Molecules. *J. Mol. Struct.*, 1006:611 – 628, 2011.

[44] L.M. Bates. Monodromy in the champagne bottle. *Zeitschrift für Angewandte Mathematik und Physik*, 42:837 – 847, 1991.

[45] R. Cushman and J. J. Duistermaat. The quantum mechanical spherical pendulum. *Bull. Am. Math. Soc.*, 19(2):475 – 479, 1988.

[46] M. S. Child, T. Weston, and J. Tennyson. Quantum monodromy in the spectrum of h₂o and other systems: New insight into the level structure of quasi-linear molecules. *Mol. Phys.*, 96:371–379, 1999.

[47] B.P. Winnewisser, M. Winnewisser, I.R. Medvedev, M. Behnke, F.C. De Lucia, S.C. Ross, and J. Koput. Experimental confirmation of quantum monodromy: The millimeter wave spectrum of cyanogen isothiocyanate ncncs. *Phys. Rev. Lett.*, 95:243002, 2005.

[48] N.F. Zobov, S.V. Shirin, O.L. Polyansky, J. Tennyson, P.-F. Coheur, P.F. Bernath, M. Carleer, and R. Colin. Monodromy in the Water Molecule. *Chem. Phys. Lett.*, 414:193 – 197, 2005.

[49] B.P. Winnewisser, M. Winnewisser, I.R. Medvedev, F.C. De Lucia, S.C. Ross, and J. Koput. Analysis of the FASSST Rotational Spectrum of NCNCS in View of Quantum Monodromy. *Phys. Chem. Chem. Phys.*, 12:8158–8189, 2010.

[50] Manfred Winnewisser, Brenda P. Winnewisser, Frank C. De Lucia, Dennis W. Tokaryk, Stephen C. Ross, and Brant E. Billinghamurst. Pursuit of Quantum Monodromy in the Far-Infrared and Mid-Infrared Spectra of NCNCS Using Synchrotron Radiation. *Phys. Chem. Chem. Phys.*, 16:17373–17407, 2014.

[51] N.J. Reilly, P.B. Changala, J.H. Baraban, D.L. Kokkin, J.F. Stanton, and M.C. McCarthy. Communication: The ground electronic state of si2c: Rovibrational level structure, quantum monodromy, and astrophysical implications. *J. Chem. Phys.*, 142:231101, 2015.

[52] F. Iachello, F. Pérez-Bernal, and P.H. Vaccaro. A Novel Algebraic Scheme for Describing Nonrigid Molecules. *Chem. Phys. Lett.*, 375:309 – 320, 2003.

[53] F. Pérez-Bernal, L.F. Santos, P.H. Vaccaro, and F. Iachello. Spectroscopic Signatures of Nonrigidity: Algebraic Analyses of Infrared and Raman Transitions in Nonrigid Species. *Chem. Phys. Lett.*, 414:398 – 404, 2005.

[54] F. Iachello and F. Pérez-bernal. Bending vibrational modes of abba molecules: Algebraic approach and its classical limit. *Mol. Phys.*, 106(2-4):223–231, 2008.

[55] F. Pérez-Bernal and L. Fortunato. Phase Diagram of Coupled Benders Within a U(3)xU(3) Algebraic Approach. *Phys. Lett. A*, 376:236 – 244, 2012.

[56] D. Larese, M.A. Caprio, F. Pérez-Bernal, and F. Iachello. A study of the bending motion in tetratomic molecules by the algebraic operator expansion method. *J. Chem. Phys.*, 140:014–304, 2014.

[57] M. Sánchez-Castellanos, R. Lemus, M. Carvajal, F. Pérez-Bernal, and J.M. Fernández. A Study of the Raman Spectrum of CO₂ Using an Algebraic Approach. *Chem. Phys. Lett.*, 554:208 – 213, 2012.

[58] M. Sánchez-Castellanos, R. Lemus, M. Carvajal, and F. Pérez-Bernal. The potential energy surface of co₂ from an algebraic approach. *International Journal of Quantum Chemistry*, 112(21):3498–3507, 2012.

[59] R. Lemus, M. Sánchez-Castellanos, F. Pérez-Bernal, J. M. Fernández, and M. Carvajal. Sim-

ulation of the raman spectra of co2: Bridging the gap between algebraic models and experimental spectra. *J. Chem. Phys.*, 141:054–306, 2014.

[60] M. Bermúdez-Montaña, M. Carvajal, F. Pérez-Bernal, and R. Lemus. An algebraic alternative for the accurate simulation of co₂ raman spectra. *J. Raman Spectrosc.*, 51:569–583, 2020.

[61] D. Larese, F. Pérez-Bernal, and F. Iachello. Signatures of Quantum Phase Transitions and Excited State Quantum Phase Transitions in the Vibrational Bending Dynamics of Triatomic Molecules. *J. Mol. Struct.*, 1051:310 – 327, 2013.

[62] B. Dietz, F. Iachello, M. Miski-Oglu, N. Pietralla, A. Richter, L. von Smekal, and J. Wambach. Lifshitz and excited-state quantum phase transitions in microwave dirac billiards. *Phys. Rev. B*, 88:104101, 2013.

[63] L. Zhao, J. Jiang, T. Tang, M. Webb, and Y. Liu. Dynamics in spinor condensates tuned by a microwave dressing field. *Phys. Rev. A*, 89:023608, 2014.

[64] J. Khalouf-Rivera, M. Carvajal, L.F. Santos, and F. Pérez-Bernal. Calculation of transition state energies in the hcn–hnc isomerization with an algebraic model. *J. Phys. Chem. A*, 123:9544–9551, 2019.

[65] J.H. Baraban, P.B. Changala, G.Ch. Mellau, J.F. Stanton, A.J. Merer, and R.W. Field. Spectroscopic characterization of isomerization transition states. *Science*, 350:1338–1342, 2015.

[66] L.F. Santos and F. Pérez-Bernal. Structure of eigenstates and quench dynamics at an excited-state quantum phase transition. *Phys. Rev. A*, 92:050101, 2015.

[67] L.F. Santos, M. Távora, and F. Pérez-Bernal. Excited-state quantum phase transitions in many-body systems with infinite-range interaction: Localization, dynamics, and bifurcation. *Phys. Rev. A*, 94:012–113, 2016.

[68] F. Pérez-Bernal and L. F. Santos. Effects of excited state quantum phase transitions on system dynamics. *Progr. Phys. Fortschr. Phys.*, 65(6-8):1600035, 2017.

[69] F.M. Izrailev. Simple Models of Quantum Chaos: Spectrum and Eigenfunctions. *Phys. Rep.*, 196:299 – 392, 1990.

[70] V. Zelevinsky, B.A. Brown, N. Frazier, and M. Horoi. The Nuclear Shell Model as a Testing Ground for Many-Body Quantum Chaos. *Phys. Rep.*, 276:85 – 176, 1996.